

# Shedding Light on Hadronization by Quarkonium Energy Correlator

An-Ping Chen,<sup>1,\*</sup> Xiaohui Liu,<sup>2,3,†</sup> and Yan-Qing Ma<sup>4,5,‡</sup>

<sup>1</sup>*College of Physics and Communication Electronics,  
Jiangxi Normal University, Nanchang 330022, China*

<sup>2</sup>*Department of Physics, Beijing Normal University, Beijing, 100875, China*

<sup>3</sup>*Key Laboratory of Multi-scale Spin Physics, Ministry of Education,  
Beijing Normal University, Beijing 100875, China*

<sup>4</sup>*School of Physics, Peking University, Beijing 100871, China*

<sup>5</sup>*Center for High Energy Physics, Peking University, Beijing 100871, China*

(Dated: May 17, 2024)

We propose to measure the energy correlator in quarkonium production, which tracks the energy deposited in the calorimeter  $\chi$ -angular distance away from the identified quarkonium. The observable eliminates the need for jets while sustaining the perturbative predictive power. Analyzing the power correction to the energy correlator, we demonstrate the novel observable supplies a unique gateway to probing the hadronization, especially when  $\cos \chi \gtrsim 0$  in the quarkonium rest frame where the perturbative emissions are depleted due to the dead-cone effects. We expect the quarkonium energy correlator to add a new dimension to quarkonium studies.

**Introduction.** — A fundamental, yet not fully understood, phenomenon in quantum chromodynamics (QCD) is color confinement. This principle asserts that the colorful quarks and gluons generated in the early universe or at the collision points of particle colliders cannot be directly observed in experiments. Instead, they undergo a process called hadronization, transforming into colorless hadrons that can be detected. The question that arises is: how does the hadronization process occur, or what precisely is the mechanism behind hadronization? Unfortunately, we do not yet have the answer, not even for the simplest question: how much energy is emitted during the hadronization process.

Heavy quarkonium, consisting of a heavy quark and a heavy antiquark pair ( $Q\bar{Q}$ ), provides an ideal system for studying the hadronization mechanism. Due to their heavy mass,  $Q\bar{Q}$  pairs cannot be produced or annihilated during the hadronization process. Therefore, the picture is straightforward: a  $Q\bar{Q}$  pair is created in a hard collision and then undergoes hadronization to form a heavy quarkonium state. To gain insight into the specifics of hadronization, it is crucial to identify the emissions that occur during this process. To this end, some observables have been extensively studied in the literature. One approach involves examining the momentum fraction of the quarkonium production within a jet [1–10]. However, this observable depends on the definition of a high transverse momentum ( $p_T$ ) jet, which can lead to the exclusion of significant data from low  $p_T$  regions. Another observable is the correlator between the quarkonium and a light hadron (or light hadrons) [11–19]. Yet, providing a reliable theoretical prediction for this correlator can pose a significant challenge because it is not infrared-safe.

In this letter, we propose a novel observable: the quarkonium-energy correlator. This observable is akin to the previously mentioned quarkonium-hadron correlator but is weighted by the energy of light hadrons, thereby

ensuring an infrared-safe property. In the helicity frame, we demonstrate that this correlator can not only probe the average energy emitted during the hadronization process but also distinguish between different production mechanisms.

**Quarkonium energy correlator.** — We consider a generic quarkonium  $\mathcal{Q}$  (e.g.,  $J/\psi$ ) production process, like in  $e^+e^-$  annihilation, hadronic collisions, or  $B$  meson decay. In addition to the quarkonium detection, we measure the total energy flow along a specific angular direction  $\chi$ , relative to the flying direction of the  $\mathcal{Q}$  but boosted into its rest frame, the so-called helicity frame. Our focus lies on measuring the *Quarkonium Energy Correlator* expressed as,

$$\Sigma(\cos \chi) = \int d\sigma \sum_i \frac{E_i}{M} \delta(\cos \chi - \cos \theta_i), \quad (1)$$

where  $d\sigma$  is the differential cross section responsible for generating the  $\mathcal{Q}$ , weighted by the total energy  $\sum_i E_i \delta(\cos \chi - \cos \theta_i)$  carried by particles propagating at the angle  $\chi$  with respect to the  $\mathcal{Q}$ . We normalize this energy to  $M$ , the mass of the quarkonium. The measurement process for  $J/\psi$  energy correlator is outlined in Fig. 1. Eq. (1) implies that the energy correlator can be understood as the average energy radiation flow directed towards the given angle  $\chi$ . Therefore by looking at the detectors placed at various  $\chi$  positions, we can explore the radiation pattern in  $\mathcal{Q}$  production through  $\Sigma(\cos \chi)$ .

In principle,  $\Sigma(\cos \chi)$  receives contributions from both hard radiation during the hard collision and non-perturbative soft radiation during the  $Q\bar{Q}$  pair transitions into the  $\mathcal{Q}$ , in the form of [20–22]

$$\Sigma(\cos \chi) = \Sigma_{P.T.}(\cos \chi) + \Sigma_{N.P.}(\cos \chi). \quad (2)$$

The energy weighting theoretically ensures the infra-red safety of the observable, enabling the calculability of

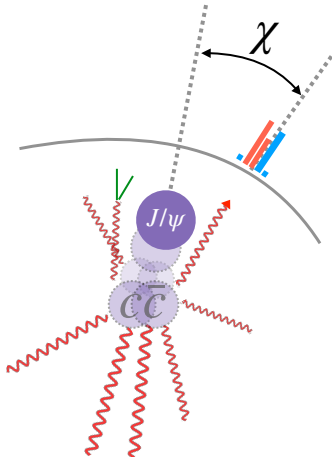


FIG. 1. Measurement of the energy correlator around the  $J/\psi$ , where the energy deposit in the calorimeter with the polar angle separation  $\chi$  from the  $J/\psi$  is recorded.

the hard radiation contribution  $\Sigma_{P.T.}$  within perturbation theory. The  $\Sigma_{P.T.}$ , as we will show, typically dominant when  $\chi \gtrsim \frac{\pi}{2}$ , can serve as a benchmark to verify the theoretical framework and the accuracy of experimental data. Meanwhile, the non-perturbative soft radiation contribution  $\Sigma_{N.P.}$  contains the physics necessary for comprehending the hadronization mechanism. As we will demonstrate in the rest of this Letter, the non-perturbative contribution  $\Sigma_{N.P.}$  could be significant when  $\chi \lesssim \frac{\pi}{2}$  compared with  $\Sigma_{P.T.}$ .

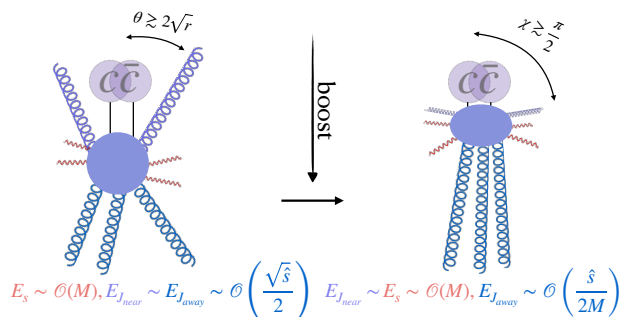


FIG. 2. Dominant configurations for hard emissions when  $\sqrt{\hat{s}} \gg M$  in the center of mass frame (left) and the quarkonium rest frame (right).

To estimate the significance of  $\Sigma_{N.P.}$ , we will first examine the scaling behavior of radiations illustrated in Fig. 2. Starting from the center of mass frame generating the  $Q + X$  (sub)-system, with an input energy  $\sqrt{\hat{s}} \gtrsim M$ , the production configuration is dominated by 2 back-to-back jets with energy  $\sim \mathcal{O}(\frac{\sqrt{\hat{s}}}{2})$  and transverse broadening  $\sim \mathcal{O}(M)$ . The inter-jet region is filled with

soft radiations with momentum  $\sim \mathcal{O}(M)$ , due to the soft and collinear feature of perturbative QCD. The collinear radiations near the quarkonium are predominantly confined to the region  $\sin \theta \gtrsim \frac{M}{\sqrt{\hat{s}/2}} \equiv 2\sqrt{r}$  due to the dead-cone effects [23, 24]. When boosted into the quarkonium rest frame, the momentum transverse to the jet axis remains unchanged. The energy of the backward jet gets magnified due to a large boost factor  $a \sim \frac{\sqrt{\hat{s}}}{M} = \sqrt{\frac{1}{r}}$  to reach  $E_{J_{away}} \sim a \frac{\sqrt{\hat{s}}}{2} = \frac{\hat{s}}{2M}$ . The energy for the collinear radiations near the quarkonium is reduced to  $E_{J_{near}} \sim \mathcal{O}(M)$ , along with the quarkonium, and the radiations are pushed to the region  $\chi \gtrsim \mathcal{O}(\frac{\pi}{2})$ . We thus expect when moving from  $\cos \chi \sim -1$  to  $\cos \chi \sim 0$ , the magnitude of  $\Sigma_{P.T.}$  drops rapidly by a factor of  $\sim \mathcal{O}(E_{J_{away}}/E_{J_{near}}) = \mathcal{O}(\frac{1}{2r})$ , and gets further suppressed as we approaching  $\cos \chi \sim 1$  since the existence of the dead-cone.

The depopulation of perturbative radiations in the  $\cos \chi > 0$  region allows  $\Sigma_{N.P.}$  to potentially outperform  $\Sigma_{P.T.}$ . Therefore, we concentrate on this region and analyze the relative importance between  $\Sigma_{N.P.}$  and  $\Sigma_{P.T.}$ . We consider three generic scenarios.

We start with considering a hard emission contributing at leading order (LO) in perturbation theory, in addition to soft emissions. In this scenario,  $\Sigma_{P.T.}$  takes precedence over  $\Sigma_{N.P.}$  due to the significantly higher energy of the hard emission, of the order  $M$ , compared to the soft emission energy scaled by  $Mv$ . Here,  $v \ll 1$  is the typical relative velocity between the  $Q\bar{Q}$  pair of the quarkonium. The precise value of the soft emission energy, a variable of great interest, depends on further exploration. For an enhanced detection of signals attributed to  $\Sigma_{N.P.}$ , it is helpful to select processes where hard emission is minimized at LO. However, it is essential to recognizing that for charmonia systems,  $v^2 \sim 0.3$  is not very small, and thus the effect of  $\Sigma_{N.P.}$  can still be observably significant even when hard emissions are present at LO.

The second case is to replace a non-perturbative soft emission with a hard emission. This is feasible because, in the language of NRQCD factorization [25], there are different production channels that can contribute to  $\Sigma(\cos \chi)$ ,

$$\Sigma(\cos \chi) = \sum_{ch} \Sigma_{P.T.}^{ch}(\cos \chi) + \Sigma_{N.P.}^{ch}(\cos \chi), \quad (3)$$

where the summation of channels  $ch$  includes the color singlet and the octet channels, proportional to their long-distance matrix elements (LDMEs), respectively. As the energy of a hard emission in one channel, such as a color-singlet channel, becomes smaller, its contribution should be transferred from the color-singlet channel to a color-octet channel as a non-perturbative emission. Because hard emission is suppressed by  $\alpha_s(M)$  and color-octet LDMEs are usually smaller than color-singlet LDMEs,

the relevant comparison in this case is between the effects of perturbative emission in the color-singlet channel and non-perturbative emission in a color-octet channel. The former scales as  $\Sigma_{P.T.}^{[1]} \lesssim \alpha_s(M) \frac{M}{M} \sigma^{[1]} \propto \alpha_s(M) \langle O_1 \rangle$ , while the latter scales as  $\Sigma_{N.P.}^{[8]} \sim \frac{Mv}{M} \sigma^{[8]} \propto v \langle O_8 \rangle$ , where  $\langle O_{1,8} \rangle$  denote color-singlet or color-octet LDMEs. For  $J/\psi$  production with the  $^1S_0^{[8]}$  channel, the velocity scaling rule gives  $v \langle O_8 \rangle \sim v^4 \langle O_1 \rangle \sim 0.1 \times \langle O_1 \rangle$  [25, 26]. Considering the  $\alpha_s(M)$  suppression and dead-cone effects for hard emission in the color-singlet channel, it is optimistic to detect the hadronization effects in the color-octet channel even if the color-singlet channel is not suppressed in the process under consideration by other mechanisms.

The last case refers to a hard emission at higher orders in perturbation theory. In this scenario, we observe the scaling behavior  $\Sigma_{P.T.} \lesssim \alpha_s(M) \frac{M}{M} \sigma$  and  $\Sigma_{N.P.} \sim \frac{Mv}{M} \sigma$ . Because  $\alpha_s(M) \ll \alpha_s(Mv) \sim v$  [25], we find that high-order perturbative effects are suppressed.

Therefore, the region where  $\cos \chi > 0$  indicates a significant area where the hadronization effect potentially plays a crucial role comparable to contributions from hard emissions. This suggests that detecting energy emitted in the hadronization process is feasible via measuring the quarkonium energy correlator in the domain  $\cos \chi > 0$ . It is important to note that these conclusions are universal in QCD and are not contingent on the particular quarkonium-producing models. To further elucidate this concept, the subsequent sections of this manuscript will provide explicit examples using  $J/\psi$  production.

**Theoretical predictions for quarkonium energy correlators.** — We first exemplify our proposal using the  $J/\psi$  production in  $e^+e^-$  annihilation,  $e^+e^- \rightarrow \gamma^* \rightarrow J/\psi + X$ . To provide a theoretical prediction, we employ the NRQCD factorization method [25], although other methods can also be used [27–33]. For this problem, the most important contributions are  $^3S_1^{[1]}$ ,  $^1S_0^{[8]}$  and  $^3P_J^{[8]}$  channels.

The leading hard process for color-singlet channel  $^3S_1^{[1]}$  is  $e^+e^- \rightarrow \gamma^* \rightarrow c\bar{c}[^3S_1^{[1]}] + g + g$ , and thus the hard emissions can contribute to the region  $\cos \chi > 0$ . The leading hard process for color-octet channel  $^1S_0^{[8]}$  or  $^3P_J^{[8]}$  is  $e^+e^- \rightarrow \gamma^* \rightarrow c\bar{c}[^1S_0^{[8]}, ^3P_J^{[8]}] + g$ , where the hard gluon and the  $c\bar{c}$  pair are back-to-back and the hard emission only contribute to  $\cos \chi = -1$ . Furthermore, soft emissions during hadronization of the color-singlet  $c\bar{c}$  pair is generally expected to be less than that of color-octet  $c\bar{c}$  pairs. Therefore, the leading  $\Sigma_{P.T.}$  comes from the  $^3S_1^{[1]}$  channel, and the leading  $\Sigma_{N.P.}$  comes from  $^1S_0^{[8]}$  and  $^3P_J^{[8]}$  channels. Based on the previous general discussion of the second case, we expect that the  $\Sigma_{N.P.}$  can be significant, as will be shown by explicit computation.

For the leading contribution for  $\Sigma_{P.T.}$ , the Eq. (1) be-

comes

$$\Sigma_{P.T.}^{^3S_1^{[1]}}(\cos \chi) = \int d\hat{\sigma}_{e^+e^- \rightarrow c\bar{c}[^3S_1^{[1]}] + g + g} \langle \mathcal{O}^{J/\psi}(^3S_1^{[1]}) \rangle \times \sum_{i=1}^2 \frac{E_i}{2m_c} \delta(\cos \chi - \cos \theta_i), \quad (4)$$

where  $d\hat{\sigma}$  is the LO partonic cross section that generates the color singlet  $c\bar{c}$  pair,  $\langle \mathcal{O}^{J/\psi}(^3S_1^{[1]}) \rangle$  is the NRQCD matrix element, and we have replaced the quarkonium mass  $M$  with  $2m_c$  in the fixed order calculation.  $\theta_i$  is the angle between directions of one gluon and the  $J/\psi$ . The analytic results can be found in the Supplemental Material (SM).

To provide an estimation for  $\Sigma_{N.P.}$ , we need to model the hadronization process from CO  $c\bar{c}$  pair to  $J/\psi$ . In NRQCD, it suggests that the transition is dominated by one soft gluon emission, while multiple emissions are sub-leading in  $v$ . If we denote the transition amplitude for  $c\bar{c}[ch] \rightarrow J/\psi + g$  as  $A^{ch}(\theta, \phi)$  with  $ch = ^1S_0^{[8]}, ^3P_J^{[8]}$ , then we find

$$\Sigma_{N.P.}^{ch}(\cos \chi) = \int d\Phi_g \frac{k^0}{M} \delta(\cos \chi - \cos \theta) \sum_{\lambda} \hat{\sigma}_{\lambda}^{ch} A_{\lambda}^{ch}(\theta, \phi), \quad (5)$$

where  $\Phi_g$  denotes the gluon phase space,  $k^0$  represents the emitted energy,  $\hat{\sigma}^{ch}$  is the total cross section that produces the  $c\bar{c}[ch]$  pair with polarization  $\lambda$ . We can see that  $\int \frac{k^0 d\phi}{16\pi^3} \sum_{ch, \lambda} \frac{\hat{\sigma}_{\lambda}^{ch}}{\sigma} A_{\lambda}^{ch}(\theta, \phi)$  characterizes the radiated energy distribution  $\rho(k_0, \theta)$  due to hadronization.

As for the  $^1S_0^{[8]}$  channel, since the intermediate  $c\bar{c}[^1S_0^{[8]}]$  state is unpolarized, the soft gluon emission should be isotropic, thus we have  $A^{^1S_0^{[8]}}(\theta, \phi) = \frac{1}{4\pi} G_0$ . Here  $G_0$  is a function of  $k^0$  but independent of  $\theta$  and  $\phi$ .  $G_0$  describes the probability of the gluon emission to form the  $J/\psi$ , therefore one should have  $\frac{1}{4\pi} \int d\Phi_g G_0 \sim \mathcal{O}(\langle \mathcal{O}^{J/\psi}(^1S_0^{[8]}) \rangle)$ . Hence, we find the hadronization contribution to the energy correlator to be isotropic with size

$$\Sigma_{N.P.}^{^1S_0^{[8]}}(\cos \chi) = \hat{\sigma}^{^1S_0^{[8]}} \int d\Phi_g \frac{k_0}{M} \frac{G_0}{4\pi} \delta(\cos \chi - \cos \theta) \equiv \bar{v}_0 \frac{\sigma^{^1S_0^{[8]}}}{4}, \quad (6)$$

where  $m_c \bar{v}_0$  parameterizes the average energy emitted during hadronization.  $\hat{\sigma}^{^1S_0^{[8]}}$  and  $\sigma^{^1S_0^{[8]}}$  is the total cross section for  $c\bar{c}[^1S_0^{[8]}]$  and the  $J/\psi$  through that  $c\bar{c}$  channel, respectively. At LO, we have  $\sigma^{^1S_0^{[8]}} = \frac{32\pi^2 \alpha^2 \alpha_s e_c^2}{3s^2 m_c} (1-r) \langle \mathcal{O}^{J/\psi}(^1S_0^{[8]}) \rangle$ . The contribution from  $^3P_J^{[8]}$  states can be obtained similarly but the calculation is more involved and we leave the details in the SM.

Fig. 3 exhibits the numerical consequence of our analysis. We set  $\sqrt{S} = 10.6$  GeV to match the Belle [34] kinematics and  $\alpha_s(\sqrt{s}/2) = 0.24$ . We use  $\langle \mathcal{O}^{J/\psi}(^3S_1^{[1]}) \rangle =$

1.16 GeV<sup>3</sup> [35]. For the CO LDMEs, we choose a set of CO LDMEs that satisfies the upper bound extraction from B factories [36]:  $\langle \mathcal{O}^{J/\psi}(^1S_0^{[8]}) \rangle = 1.0 \times 10^{-2} \text{ GeV}^3$ , and  $\langle \mathcal{O}^{J/\psi}(^3P_0^{[8]}) \rangle / m_c^2 = 0.25 \times 10^{-2} \text{ GeV}^3$ . To evaluate  $\Sigma_{N.P.}$ , we tentatively set  $\bar{v}_0^2 = \bar{v}_1^2 = 0.25$  consistent with NRQCD power counting for charmonia, while its true value should be determined by future experimental analysis.

The dash-dotted line in black in Fig. 3 shows the LO  $^3S_1^{[1]}$  contribution to the  $\Sigma(\cos\chi)$ . We can see that the radiations in the color singlet contribution occupy dominantly around  $\chi \sim \pi$  and drop significantly when  $\chi \lesssim \frac{\pi}{2}$ , which coincides with our previous analysis. Based on our previous analysis, we do not expect the shape in  $\chi \lesssim \frac{\pi}{2}$  to change substantially when including higher-order corrections.

The suppression of the hard radiation raises the chance to probe the nonperturbative hadronization contribution when  $\chi \lesssim \frac{\pi}{2}$ . Indeed, as manifest in Fig. 3, the hadronization contribution, shown in the blue line, is about the same size as the  $\Sigma_{P.T.}$ , making the hadronization effect detectable at the currently available Belle experiment [37].

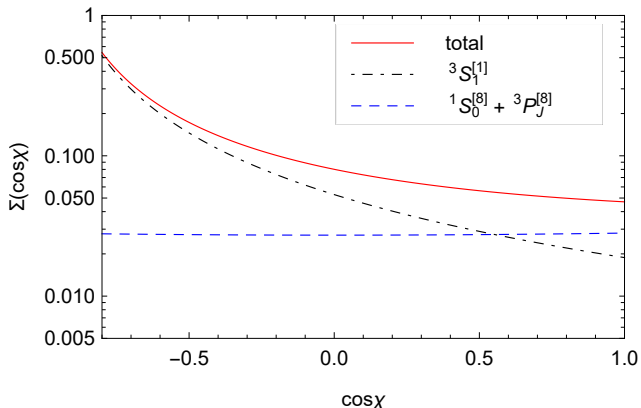


FIG. 3. Theoretical predictions for  $J/\psi$  energy correlator in  $e^+e^-$  collision with  $\sqrt{S} = 10.6$  GeV.

Now we show the energy correlation in  $pp$  collisions. For illustration, we consider  $J/\psi$  production at high  $p_T$  and simplify our analysis using single-gluon fragmentation framework, in which

$$\Sigma(\cos\chi) = \sum_n \int_0^1 dz d\hat{\sigma}_{A+B \rightarrow g+X}(\hat{p}/z, \mu_F) \times \hat{D}_{g \rightarrow c\bar{c}[n]}(z, \cos\chi, \mu_F) \langle \mathcal{O}^{J/\psi}(n) \rangle. \quad (7)$$

The notations and the derivation can be found in the SM. Since we are mostly interested in the region  $\cos\chi > 0$ , for illustrative purposes, we have ignored the contribution to  $\Sigma(\cos\chi)$  from the short coefficient  $\hat{\sigma}_{A+B \rightarrow g+X}$

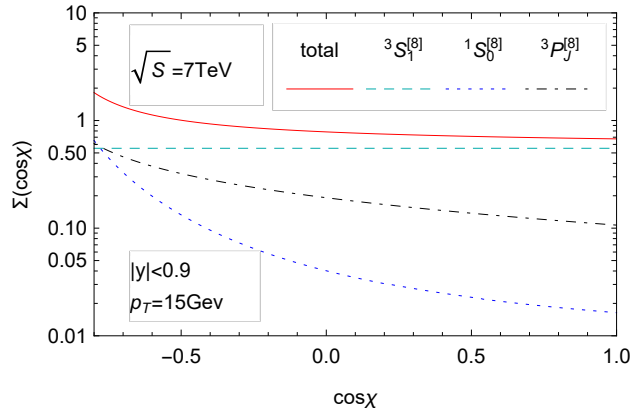


FIG. 4. Theoretical predictions for  $J/\psi$  energy correlator in  $pp$  collision with  $p_T = 15$  GeV at  $\sqrt{S} = 7$  TeV and  $|y| < 0.9$ . Contribution from the short-distance coefficient  $\hat{\sigma}_{A+B \rightarrow g+X}$  is not included in this prediction.

which typically contributes to  $\cos\chi < 0$ . A complete analysis will be presented in future publication. The numerical results are exhibited in Fig. 4, obtained with  $p_T = 15$  GeV and  $|y| < 0.9$  at  $\sqrt{S} = 7$  TeV. Here  $\Sigma_{P.T.}$  receives dominant contributions from the  $^1S_0^{[8]}$  and  $^3P_J^{[8]}$  channels, and  $\Sigma_{N.P.}$  from the  $^3S_1^{[8]}$  channel. We used the LDMEs from the fit of Ref.[38]:  $\langle \mathcal{O}^{J/\psi}(^1S_0^{[8]}) \rangle = 8.9 \times 10^{-2} \text{ GeV}^3$ ,  $\langle \mathcal{O}^{J/\psi}(^3P_0^{[8]}) \rangle / m_c^2 = 0.56 \times 10^{-2} \text{ GeV}^3$ , and  $\langle \mathcal{O}^{J/\psi}(^3S_1^{[8]}) \rangle = 0.3 \times 10^{-2} \text{ GeV}^3$ , and we have set  $\bar{v}_2^2 = 0.25$ . The calculated  $\Sigma_{P.T.}$  supports our previous analysis based on the generic properties of QCD. A significant  $\Sigma_{N.P.}$  is observed from the  $^3S_1^{[8]}$  channel in our current predictions. This is because the partonic cross-section  $d\hat{\sigma}_{A+B \rightarrow g+X} \sim z^4$  [39, 40]. Consequently, the energy correlator effectively scales as the 4th moment of the fragmentation functions (FFs)  $\hat{D}_{g \rightarrow c\bar{c}[n]}$ . Compared to the LO NRQCD  $^3S_1^{[8]}$  FF, which is proportional to  $\delta(1-z)$ , the  $^1S_0^{[8]}$  FF peaks at  $z = 0$  and the  $^3P_J^{[8]}$  FF gradually increases as  $z \rightarrow 1$ . Therefore when convoluted with  $d\hat{\sigma}_{A+B \rightarrow g+X}$ , the contribution from  $^1S_0^{[8]}$  and  $^3P_J^{[8]}$  are significantly suppressed, compared with  $^3S_1^{[8]}$ . Relativistic corrections at higher orders will soften and migrate the peak in the  $^3S_1^{[8]}$  FF to lower values of  $z$  and hence reduce the estimated  $\Sigma_{N.P.}$  size. For a more reliable estimation, one can apply the soft gluon factorization [33] to account for higher order relativistic corrections, and find the hadronization effect is reduced by a fact of 60%, yet the size remains detectable for future studies.

To enclose the section, we note that our prediction assumes the rotational covariance of the non-perturbative radiations as required by the NRQCD factorization theorem. Although this assumption has been explicitly veri-

fied up to 2-loop order [41, 42]<sup>1</sup>, the rotational covariance of the NRQCD soft emission necessitates further testing and verification. The quarkonium energy correlator provides the possibility to probe the distribution of the soft radiations experimentally. For instance, instead of rotational covariance, if the soft radiation is boost-covariant, which is the case where the soft radiation relies explicitly on the direction of a Wilson line [43], we may expect  $\Sigma_{N.P.} \sim \frac{1}{\sin^3 \chi}$  similar to light hadron energy-energy correlator [20–22] and experiences significant amplification as  $\chi \rightarrow 0$ , which is distinct from the expectation based on the rotational covariance assumption. As a result, future experiments could differentiate between these distributions through a refined measurement near  $\chi = 0$  in the quarkonium energy correlator spectrum.

**Summary and outlook.** — In this Letter, we proposed the quarkonium-energy correlator which extends the concept of the energy correlators [44–86] to heavy quarkonium studies. The quarkonium energy correlator measures the energy flow at an angle distance  $\chi$  away from the quarkonium in its rest frame. Notably, for generic  $J/\psi$  production, such as at the Belle experiment or the LHC, we demonstrate that the hadronization effect leads to comparable power correction to the energy correlator relative to the perturbative hard radiations in the region where  $\cos \chi \gtrsim 0$  due to the compelling dead-cone effects. Our explicit calculations manifest the statement, further showing its potential to unveil the hadronization mechanisms in heavy quarkonium production. We thus expect the energy correlator the exceptional observable to offer unprecedented insights into the complex non-perturbative phenomena governing heavy quarkonium production.

**Acknowledgments.** — The work was supported in part by the National Natural Science Foundation of China (No. 12325503, No. 12205124), the National Key Research and Development Program of China under Contract No. 2020YFA0406400, and the High-performance Computing Platform of Peking University. X. L. is supported by the Natural Science Foundation of China under Contract No. 12175016.

---

\* chenanning@jxnu.edu.cn

† xiliu@bnu.edu.cn

‡ yqma@pku.edu.cn

[1] M. Baumgart, A. K. Leibovich, T. Mehen, and I. Z. Rothstein, *Probing Quarkonium Production*

*Mechanisms with Jet Substructure*, *JHEP* **11** (2014) 003 [arXiv:1406.2295] [InSPIRE].

- [2] R. Bain, L. Dai, A. Hornig, A. K. Leibovich, Y. Makris, and T. Mehen, *Analytic and Monte Carlo Studies of Jets with Heavy Mesons and Quarkonia*, *JHEP* **06** (2016) 121 [arXiv:1603.06981] [InSPIRE].
- [3] Z.-B. Kang, J.-W. Qiu, F. Ringer, H. Xing, and H. Zhang,  *$J/\psi$  production and polarization within a jet*, *Phys. Rev. Lett.* **119** (2017) 032001 [arXiv:1702.03287] [InSPIRE].
- [4] R. Bain, L. Dai, A. Leibovich, Y. Makris, and T. Mehen, *NRQCD Confronts LHCb Data on Quarkonium Production within Jets*, *Phys. Rev. Lett.* **119** (2017) 032002 [arXiv:1702.05525] [InSPIRE].
- [5] S.-L. Zhang and H. Xing,  *$J/\psi$  production within a jet in high-energy proton-proton and nucleus-nucleus collisions*, [arXiv:2403.12704] [InSPIRE].
- [6] **LHCb**, R. Aaij *et al.*, *Study of  $J/\psi$  Production in Jets*, *Phys. Rev. Lett.* **118** (2017) 192001 [arXiv:1701.05116] [InSPIRE].
- [7] **LHCb**, R. Aaij *et al.*, *Observation of Multiplicity Dependent Prompt  $\chi_{c1}(3872)$  and  $\psi(2S)$  Production in  $pp$  Collisions*, *Phys. Rev. Lett.* **126** (2021) 092001 [arXiv:2009.06619] [InSPIRE].
- [8] **CMS**, A. M. Sirunyan *et al.*, *Study of  $J/\psi$  meson production inside jets in  $pp$  collisions at  $\sqrt{s} = 8$  TeV*, *Phys. Lett. B* **804** (2020) 135409 [arXiv:1910.01686] [InSPIRE].
- [9] **CMS**, A. Tumasyan *et al.*, *Fragmentation of jets containing a prompt  $J/\psi$  meson in PbPb and  $pp$  collisions at  $\sqrt{s_{NN}} = 5.02$  TeV*, *Phys. Lett. B* **825** (2022) 136842 [arXiv:2106.13235] [InSPIRE].
- [10] Q. Yang,  *$J/\psi$  production within a jet in  $p+p$  collisions at  $\sqrt{s} = 500$  GeV by STAR*, *PoS HardProbes2020* (2021) 072.
- [11] **UA1**, C. Albajar *et al.*, *High Transverse Momentum  $J/\psi$  Production at the CERN Proton - Anti-proton Collider*, *Phys. Lett. B* **200** (1988) 380–390 [InSPIRE].
- [12] **UA1**, C. Albajar *et al.*,  *$J/\psi$  and  $\psi'$  production at the CERN  $p$  anti- $p$  collider*, *Phys. Lett. B* **256** (1991) 112–120 [InSPIRE].
- [13] S. Porteboeuf and R. Granier de Cassagnac,  *$J/\Psi$  yield vs. multiplicity in proton-proton collisions at the LHC*, *Nucl. Phys. B Proc. Suppl.* **214** (2011) 181–184 [arXiv:1012.0719] [InSPIRE].
- [14] **ALICE**, B. Abelev *et al.*,  *$J/\psi$  Production as a Function of Charged Particle Multiplicity in  $pp$  Collisions at  $\sqrt{s} = 7$  TeV*, *Phys. Lett. B* **712** (2012) 165–175 [arXiv:1202.2816] [InSPIRE].
- [15] **CMS**, S. Chatrchyan *et al.*, *Event Activity Dependence of  $\Upsilon(nS)$  Production in  $\sqrt{s_{NN}}=5.02$  TeV  $pPb$  and  $\sqrt{s}=2.76$  TeV  $pp$  Collisions*, *JHEP* **04** (2014) 103 [arXiv:1312.6300] [InSPIRE].
- [16] **CMS**, V. Khachatryan *et al.*,  *$\Upsilon(nS)$  polarizations versus particle multiplicity in  $pp$  collisions at  $\sqrt{s} = 7$  TeV*, *Phys. Lett. B* **761** (2016) 31–52 [arXiv:1603.02913] [InSPIRE].
- [17] **STAR**, J. Adam *et al.*,  *$J/\psi$  production cross section and its dependence on charged-particle multiplicity in  $p + p$  collisions at  $\sqrt{s} = 200$  GeV*, *Phys. Lett. B* **786** (2018) 87–93 [arXiv:1805.03745] [InSPIRE].
- [18] **ALICE**, S. Acharya *et al.*, *Measurement of  $\psi(2S)$  production as a function of charged-particle pseudorapidity density in  $pp$  collisions at  $\sqrt{s} = 13$  TeV*

---

<sup>1</sup> We also note that the check relies on an inclusive integration over the soft gluon phase space. For a generic observable that restricts the soft radiation phase space, the conclusion may already not apply.

- and  $p$ - $Pb$  collisions at  $\sqrt{s_{NN}} = 8.16$  TeV with ALICE at the LHC, *JHEP* **06** (2023) 147 [arXiv:2204.10253] [InSPIRE].
- [19] J.-P. Lansberg, *New Observables in Inclusive Production of Quarkonia*, *Phys. Rept.* **889** (2020) 1–106 [arXiv:1903.09185] [InSPIRE].
- [20] G. P. Korchemsky and G. F. Sterman, *Power corrections to event shapes and factorization*, *Nucl. Phys. B* **555** (1999) 335–351 [hep-ph/9902341] [InSPIRE].
- [21] A. V. Belitsky, G. P. Korchemsky, and G. F. Sterman, *Energy flow in QCD and event shape functions*, *Phys. Lett. B* **515** (2001) 297–307 [hep-ph/0106308] [InSPIRE].
- [22] S. T. Schindler, I. W. Stewart, and Z. Sun, *Renormalons in the energy-energy correlator*, *JHEP* **10** (2023) 187 [arXiv:2305.19311] [InSPIRE].
- [23] Y. L. Dokshitzer, V. A. Khoze, and S. I. Troian, *On specific QCD properties of heavy quark fragmentation ('dead cone')*, *J. Phys. G* **17** (1991) 1602–1604 [InSPIRE].
- [24] ALICE, S. Acharya *et al.*, *Direct observation of the dead-cone effect in quantum chromodynamics*, *Nature* **605** (2022) 440–446 [arXiv:2106.05713] [InSPIRE]. [Erratum: Nature 607, E22 (2022)].
- [25] G. T. Bodwin, E. Braaten, and G. P. Lepage, *Rigorous QCD analysis of inclusive annihilation and production of heavy quarkonium*, *Phys. Rev. D* **51** (1995) 1125–1171 [hep-ph/9407339] [InSPIRE]. [Erratum: Phys.Rev.D 55, 5853 (1997)].
- [26] G. T. Bodwin, U.-R. Kim, and J. Lee, *Higher-order relativistic corrections to gluon fragmentation into spin-triplet  $S$ -wave quarkonium*, *JHEP* **11** (2012) 020 [arXiv:1208.5301] [InSPIRE]. [Erratum: JHEP 07, 170 (2023)].
- [27] S. D. Ellis, M. B. Einhorn, and C. Quigg, *Comment on Hadronic Production of Psions*, *Phys. Rev. Lett.* **36** (1976) 1263 [InSPIRE].
- [28] C. E. Carlson and R. Suaya, *Hadronic Production of  $\psi$ / $J$  Mesons*, *Phys. Rev. D* **14** (1976) 3115 [InSPIRE].
- [29] C.-H. Chang, *Hadronic Production of  $J/\psi$  Associated With a Gluon*, *Nucl. Phys. B* **172** (1980) 425–434 [InSPIRE].
- [30] H. Fritzsche, *Producing Heavy Quark Flavours in Hadronic Collisions: A Test of Quantum Chromodynamics*, *Phys. Lett. B* **67** (1977) 217–221 [InSPIRE].
- [31] F. Halzen, *Cvc for Gluons and Hadroproduction of Quark Flavours*, *Phys. Lett. B* **69** (1977) 105–108 [InSPIRE].
- [32] Y.-Q. Ma and R. Vogt, *Quarkonium Production in an Improved Color Evaporation Model*, *Phys. Rev. D* **94** (2016) 114029 [arXiv:1609.06042] [InSPIRE].
- [33] Y.-Q. Ma and K.-T. Chao, *New factorization theory for heavy quarkonium production and decay*, *Phys. Rev. D* **100** (2019) 094007 [arXiv:1703.08402] [InSPIRE].
- [34] Belle, P. Pakhlov *et al.*, *Measurement of the  $e^+e^- \rightarrow J/\psi c$  anti- $c$  cross section at  $s^{*(1/2)} \sim 10.6$ -GeV*, *Phys. Rev. D* **79** (2009) 071101 [arXiv:0901.2775] [InSPIRE].
- [35] E. J. Eichten and C. Quigg, *Quarkonium wave functions at the origin*, *Phys. Rev. D* **52** (1995) 1726–1728 [hep-ph/9503356] [InSPIRE].
- [36] Y.-J. Zhang, Y.-Q. Ma, K. Wang, and K.-T. Chao, *QCD radiative correction to color-octet  $J/\psi$  inclusive production at  $B$  Factories*, *Phys. Rev. D* **81** (2010) 034015 [arXiv:0911.2166] [InSPIRE].
- [37] Belle-II, W. Altmannshofer *et al.*, *The Belle II Physics Book*, *PTEP* **2019** (2019) 123C01 [arXiv:1808.10567] [InSPIRE]. [Erratum: PTEP 2020, 029201 (2020)].
- [38] K.-T. Chao, Y.-Q. Ma, H.-S. Shao, K. Wang, and Y.-J. Zhang,  *$J/\psi$  Polarization at Hadron Colliders in Nonrelativistic QCD*, *Phys. Rev. Lett.* **108** (2012) 242004 [arXiv:1201.2675] [InSPIRE].
- [39] M. L. Mangano and A. Petrelli, *NLO quarkonium production in hadronic collisions*, *Int. J. Mod. Phys. A* **12** (1997) 3887–3897 [hep-ph/9610364] [InSPIRE].
- [40] G. T. Bodwin, K.-T. Chao, H. S. Chung, U.-R. Kim, J. Lee, and Y.-Q. Ma, *Fragmentation contributions to hadroproduction of prompt  $J/\psi$ ,  $\chi_{cJ}$ , and  $\psi(2S)$  states*, *Phys. Rev. D* **93** (2016) 034041 [arXiv:1509.07904] [InSPIRE].
- [41] J. P. Ma and Z. G. Si, *NRQCD factorization and universality of NRQCD matrix elements*, *Phys. Lett. B* **625** (2005) 67–75 [hep-ph/0506078] [InSPIRE].
- [42] G. C. Nayak, J.-W. Qiu, and G. F. Sterman, *NRQCD Factorization and Velocity-dependence of NNLO Poles in Heavy Quarkonium Production*, *Phys. Rev. D* **74** (2006) 074007 [hep-ph/0608066] [InSPIRE].
- [43] G. C. Nayak, J.-W. Qiu, and G. F. Sterman, *Fragmentation, factorization and infrared poles in heavy quarkonium production*, *Phys. Lett. B* **613** (2005) 45–51 [hep-ph/0501235] [InSPIRE].
- [44] C. Basham, L. S. Brown, S. D. Ellis, and S. T. Love, *Energy Correlations in electron - Positron Annihilation: Testing QCD*, *Phys. Rev. Lett.* **41** (1978) 1585 [InSPIRE].
- [45] C. Basham, L. Brown, S. Ellis, and S. Love, *Energy Correlations in electron-Positron Annihilation in Quantum Chromodynamics: Asymptotically Free Perturbation Theory*, *Phys. Rev. D* **19** (1979) 2018 [InSPIRE].
- [46] D. M. Hofman and J. Maldacena, *Conformal collider physics: Energy and charge correlations*, *JHEP* **05** (2008) 012 [arXiv:0803.1467] [InSPIRE].
- [47] A. Belitsky, S. Hohenegger, G. Korchemsky, E. Sokatchev, and A. Zhiboedov, *Energy-Energy Correlations in  $N=4$  Supersymmetric Yang-Mills Theory*, *Phys. Rev. Lett.* **112** (2014) 071601 [arXiv:1311.6800] [InSPIRE].
- [48] A. Belitsky, S. Hohenegger, G. Korchemsky, E. Sokatchev, and A. Zhiboedov, *From correlation functions to event shapes*, *Nucl. Phys. B* **884** (2014) 305–343 [arXiv:1309.0769] [InSPIRE].
- [49] M. Kologlu, P. Kravchuk, D. Simmons-Duffin, and A. Zhiboedov, *The light-ray OPE and conformal colliders*, *JHEP* **01** (2021) 128 [arXiv:1905.01311] [InSPIRE].
- [50] G. Korchemsky, *Energy correlations in the end-point region*, *JHEP* **01** (2020) 008 [arXiv:1905.01444] [InSPIRE].
- [51] L. J. Dixon, I. Moulton, and H. X. Zhu, *Collinear limit of the energy-energy correlator*, *Phys. Rev. D* **100** (2019) 014009 [arXiv:1905.01310] [InSPIRE].
- [52] H. Chen, M.-X. Luo, I. Moulton, T.-Z. Yang, X. Zhang, and H. X. Zhu, *Three point energy correlators in the collinear limit: symmetries, dualities and analytic*

- results, *JHEP* **08** (2020) 028 [arXiv:1912.11050] [InSPIRE].
- [53] D. Chicherin, J. M. Henn, E. Sokatchev, and K. Yan, *From correlation functions to event shapes in QCD*, *JHEP* **02** (2021) 053 [arXiv:2001.10806] [InSPIRE].
- [54] H. Chen, I. Moulton, and H. X. Zhu, *Quantum Interference in Jet Substructure from Spinning Gluons*, *Phys. Rev. Lett.* **126** (2021) 112003 [arXiv:2011.02492] [InSPIRE].
- [55] H. Chen, I. Moulton, X. Zhang, and H. X. Zhu, *Rethinking jets with energy correlators: Tracks, resummation, and analytic continuation*, *Phys. Rev. D* **102** (2020) 054012 [arXiv:2004.11381] [InSPIRE].
- [56] C.-H. Chang, M. Kologlu, P. Kravchuk, D. Simmons-Duffin, and A. Zhiboedov, *Transverse spin in the light-ray OPE*, *JHEP* **05** (2022) 059 [arXiv:2010.04726] [InSPIRE].
- [57] Y. Li, I. Moulton, S. S. van Velzen, W. J. Waalewijn, and H. X. Zhu, *Extending Precision Perturbative QCD with Track Functions*, *Phys. Rev. Lett.* **128** (2022) 182001 [arXiv:2108.01674] [InSPIRE].
- [58] M. Jaarsma, Y. Li, I. Moulton, W. J. Waalewijn, and H. X. Zhu, *Renormalization group flows for track function moments*, *JHEP* **06** (2022) 139 [arXiv:2201.05166] [InSPIRE].
- [59] P. T. Komiske, I. Moulton, J. Thaler, and H. X. Zhu, *Analyzing N-point Energy Correlators Inside Jets with CMS Open Data*, [arXiv:2201.07800] [InSPIRE].
- [60] J. Holguin, I. Moulton, A. Pathak, and M. Procura, *A New Paradigm for Precision Top Physics: Weighing the Top with Energy Correlators*, [arXiv:2201.08393] [InSPIRE].
- [61] K. Yan and X. Zhang, *Three-Point Energy Correlator in  $N=4$  Supersymmetric Yang-Mills Theory*, *Phys. Rev. Lett.* **129** (2022) 021602 [arXiv:2203.04349] [InSPIRE].
- [62] H. Chen, I. Moulton, J. Sandor, and H. X. Zhu, *Celestial Blocks and Transverse Spin in the Three-Point Energy Correlator*, [arXiv:2202.04085] [InSPIRE].
- [63] C.-H. Chang and D. Simmons-Duffin, *Three-point energy correlators and the celestial block expansion*, [arXiv:2202.04090] [InSPIRE].
- [64] H. Chen, I. Moulton, J. Thaler, and H. X. Zhu, *Non-Gaussianities in collider energy flux*, *JHEP* **07** (2022) 146 [arXiv:2205.02857] [InSPIRE].
- [65] K. Lee, B. Meçaj, and I. Moulton, *Conformal Colliders Meet the LHC*, [arXiv:2205.03414] [InSPIRE].
- [66] X. Liu and H. X. Zhu, *Nucleon Energy Correlators*, *Phys. Rev. Lett.* **130** (2023) 091901 [arXiv:2209.02080] [InSPIRE].
- [67] L. Ricci and M. Riembau, *Energy Correlators of Hadronically Decaying Electroweak Bosons*, [arXiv:2207.03511] [InSPIRE].
- [68] T.-Z. Yang and X. Zhang, *Analytic Computation of Three-point Energy Correlator in QCD*, [arXiv:2208.01051] [InSPIRE].
- [69] C. Andres, F. Dominguez, R. Kunnawalkam Elayavalli, J. Holguin, C. Marquet, and I. Moulton, *Resolving the Scales of the Quark-Gluon Plasma with Energy Correlators*, [arXiv:2209.11236] [InSPIRE].
- [70] E. Craft, K. Lee, B. Meçaj, and I. Moulton, *Beautiful and Charming Energy Correlators*, [arXiv:2210.09311] [InSPIRE].
- [71] H. Chen, M. Jaarsma, Y. Li, I. Moulton, W. J. Waalewijn, and H. X. Zhu, *Multi-Collinear Splitting Kernels for Track Function Evolution*, [arXiv:2210.10058] [InSPIRE].
- [72] H.-Y. Liu, X. Liu, J.-C. Pan, F. Yuan, and H. X. Zhu, *Nucleon Energy Correlators for the Color Glass Condensate*, *Phys. Rev. Lett.* **130** (2023) 181901 [arXiv:2301.01788] [InSPIRE].
- [73] X. L. Li, X. Liu, F. Yuan, and H. X. Zhu, *Illuminating nucleon-gluon interference via calorimetric asymmetry*, *Phys. Rev. D* **108** (2023) L091502 [arXiv:2308.10942] [InSPIRE].
- [74] C. Andres, F. Dominguez, J. Holguin, C. Marquet, and I. Moulton, *A coherent view of the quark-gluon plasma from energy correlators*, *JHEP* **09** (2023) 088 [arXiv:2303.03413] [InSPIRE].
- [75] K. Devereaux, W. Fan, W. Ke, K. Lee, and I. Moulton, *Imaging Cold Nuclear Matter with Energy Correlators*, [arXiv:2303.08143] [InSPIRE].
- [76] C. Andres, F. Dominguez, J. Holguin, C. Marquet, and I. Moulton, *Seeing Beauty in the Quark-Gluon Plasma with Energy Correlators*, [arXiv:2307.15110] [InSPIRE].
- [77] M. Jaarsma, Y. Li, I. Moulton, W. J. Waalewijn, and H. X. Zhu, *Energy correlators on tracks: resummation and non-perturbative effects*, *JHEP* **12** (2023) 087 [arXiv:2307.15739] [InSPIRE].
- [78] K. Lee and I. Moulton, *Energy Correlators Taking Charge*, [arXiv:2308.00746] [InSPIRE].
- [79] K. Lee and I. Moulton, *Joint Track Functions: Expanding the Space of Calculable Correlations at Colliders*, [arXiv:2308.01332] [InSPIRE].
- [80] Z. Yang, Y. He, I. Moulton, and X.-N. Wang, *Probing the Short-Distance Structure of the Quark-Gluon Plasma with Energy Correlators*, *Phys. Rev. Lett.* **132** (2024) 011901 [arXiv:2310.01500] [InSPIRE].
- [81] H. Chen, *QCD factorization from light-ray OPE*, *JHEP* **01** (2024) 035 [arXiv:2311.00350] [InSPIRE].
- [82] J. Holguin, I. Moulton, A. Pathak, M. Procura, R. Schöfbeck, and D. Schwarz, *Using the W as a Standard Candle to Reach the Top: Calibrating Energy Correlator Based Top Mass Measurements*, [arXiv:2311.02157] [InSPIRE].
- [83] H. Cao, H. T. Li, and Z. Mi, *Bjorken x weighted Energy-Energy Correlators from the Target Fragmentation Region to the Current Fragmentation Region*, [arXiv:2312.07655] [InSPIRE].
- [84] A. Gao, H. T. Li, I. Moulton, and H. X. Zhu, *The Transverse Energy-Energy Correlator at Next-to-Next-to-Next-to-Leading Logarithm*, [arXiv:2312.16408] [InSPIRE].
- [85] T.-Z. Yang and X. Zhang, *Three-point Energy Correlators in Hadronic Higgs Decays*, [arXiv:2402.05174] [InSPIRE].
- [86] X. Liu and H. X. Zhu, *TMDs from Semi-inclusive Energy Correlators*, [arXiv:2403.08874] [InSPIRE].
- [87] W.-Y. Keung, *Off Resonance Production of Heavy Vector Quarkonium States in  $e^+e^-$  Annihilation*, *Phys. Rev. D* **23** (1981) 2072 [InSPIRE].
- [88] F. Yuan, C.-F. Qiao, and K.-T. Chao, *Prompt  $J/\psi$  production at  $e^+e^-$  colliders*, *Phys. Rev. D* **56** (1997) 321–328 [hep-ph/9703438] [InSPIRE].
- [89] P. L. Cho, M. B. Wise, and S. P. Trivedi, *Gluon fragmentation into polarized charmonium*, *Phys. Rev. D* **51** (1995) R2039–R2043 [hep-ph/9408352] [InSPIRE].

Supplemental Materials for ‘‘Shedding Light on Hadronization by Quarkonium Energy Correlator’’

Quarkonium Energy Correlator in  $e^+e^-$  annihilation

We present analytic results for the energy correlator measured in the  $J/\psi$  leptonic production. Following Eq. (4), we boost  $J/\psi$  to its rest frame, and

$$\cos \theta_i = \frac{1}{\sqrt{z^2 - 4r}} \left( \frac{2x_i}{z_i} - z \right), \quad (8)$$

where  $r = \frac{4m_c^2}{s}$  with  $\sqrt{s}$  the machine center of mass energy, and we have introduced the dimensionless variables  $z = \frac{2p \cdot q}{s}$ ,  $x_i = \frac{2k_i \cdot q}{s}$ ,  $z_i = \frac{2k_i \cdot p}{4m_c^2}$ , with  $q$ ,  $p$  and  $k_i$  the momentum of the virtual photon, the  $c\bar{c}$  pair and the out-going gluons, respectively.

The phase space integration in Eq. (4) can be parameterized in terms of  $x_1$  and  $z$ , which gives

$$\begin{aligned} \Sigma_{P.T.}^{3S_1^{[1]}}(\cos \chi) &= \frac{256\pi e_c^2 \alpha^2 \alpha_s^2}{81s} \frac{\mathcal{O}^{J/\psi}(3S_1^{[1]})}{(2m_c)^3} r^2 \\ &\times \int_{2\sqrt{r}}^{1+r} dz \int_{x_-}^{x_+} dx_1 f(z, x_1) \sum_{i=1}^2 \frac{z_i}{2} \delta(\cos \chi - \cos \theta_i), \end{aligned} \quad (9)$$

where we have replaced  $E_i/(2m_c)$  in the  $J/\psi$  rest frame by  $z_i/2$ , with  $z_1 = \frac{1}{2r}(x_1 - x_2 + z - 2r)$ ,  $z_2 = \frac{1}{2r}(x_2 - x_1 + z - 2r)$ ,  $x_2 = 2 - x_1 - z$ ,  $x_{\pm} = \frac{1}{2}(2 - z \pm \sqrt{z^2 - 4r})$  and

$$\begin{aligned} f(z, x_1) &= \frac{1}{(2-z)^2} \left( \frac{1}{r} + \frac{(2+x_1)x_1}{(1-x_2-r)^2} + \frac{(2+x_2)x_2}{(1-x_1-r)^2} \right. \\ &+ \frac{2(1-z)(1-r)}{r(1-x_2-r)(1-x_1-r)} + \frac{(2-z)^2((z-r)^2-1)}{(1-x_2-r)^2(1-x_1-r)^2} \\ &\left. + \frac{6(1+r-z)^2}{(1-x_2-r)^2(1-x_1-r)^2} \right), \end{aligned} \quad (10)$$

is known in the literature [87, 88]. Evaluating Eq. (9) finds the LO color singlet contribution to the energy correlator.

The non-perturbative  $\Sigma_{N.P.}$  also receives a contribution from the  $^3P_J^{[8]}$  states where, at the leading order in  $v$ , a  $c\bar{c}[^3P_J^{[8]}]$  pair with  $S = 1$  and  $L = 1$  is transmitted into the  $J/\psi$  through one electrical dipole ( $E_1$ ) interaction. Since we are measuring the polar  $\chi$  angle, different helicity and angular momentum states contribute differently. Following [89] and using the heavy quark spin symmetry, we find

$$A_T^{3P_J^{[8]}}(\theta, \phi) = \frac{3(1 + \cos^2 \theta)}{16\pi} G_1, \quad (11a)$$

$$A_L^{3P_J^{[8]}}(\theta, \phi) = \frac{3(1 - \cos^2 \theta)}{8\pi} G_1, \quad (11b)$$

where the subscripts  $T$  and  $L$  stand for the  $z$ -component of the  $c\bar{c}$ -pair’s orbital angular momentum  $|L_z| = 1$  and 0, respectively.  $G_1$  is solid angle independent and satisfies  $\frac{1}{4\pi} \int d\Phi_g G_1 \sim \mathcal{O}(\langle \mathcal{O}^{J/\psi}(^3P_0^{[8]}) \rangle)$ . We then derived the hadronization in the  $^3P_J^{[8]}$  channel to be

$$\begin{aligned} \Sigma_{N.P.}^{3P_J^{[8]}}(\cos \chi) &= \int d\Phi_g \frac{k^0}{M} \frac{G_1}{2\pi} \delta(\cos \chi - \cos \theta) \times 3 \left( \frac{1 + \cos^2 \theta}{8} \hat{\sigma}_T^{3P_0^{[8]}} + \frac{1 - \cos^2 \theta}{4} \hat{\sigma}_L^{3P_0^{[8]}} \right) \\ &\equiv \bar{v}_1 \times 3 \left( \frac{1 + \cos^2 \chi}{16} \sigma_T^{3P_0^{[8]}} + \frac{1 - \cos^2 \chi}{8} \sigma_L^{3P_0^{[8]}} \right). \end{aligned} \quad (12)$$

Here  $m_c \bar{v}_1$  is the average emitted and the  $J/\psi$  total production cross section is given by

$$\sigma_T^{3P_0^{[8]}} = -F \frac{2}{(1-r)^4} \left( 3r^5 + r^4 + 12r^3 - 16r^2 - 4(r^2 + 3r + 2)r^2 \ln r + r - 1 \right), \quad (13a)$$



$$\sigma_L^{3P_0^{[8]}} = -F \frac{1+r}{(1-r)^4} \left( r^4 - 22r^3 + 16r^2 + 8(r+2)r^2 \ln r + 6r - 1 \right), \quad (13b)$$

with  $F = \frac{32\pi^2 \alpha_s^2 e_c^2}{3s^2 m_c^3} \langle \mathcal{O}^{J/\psi}(3P_0^{[8]}) \rangle$ . We notice that when  $r \rightarrow 0$ ,  $\sigma_T^{3P_0^{[8]}} \rightarrow 2\sigma_L^{3P_0^{[8]}}$ , and in this limit the  $\chi$  dependence tends to drop out.

### Quarkonium Energy Correlator in $pp$ collisions

Similar measurements can be carried out in  $pp$  collisions. For illustration, we simplify our analysis by assuming that the  $J/\psi$  is predominantly produced through the gluon fragmentation

$$d\sigma_{A+B \rightarrow J/\psi+X}(p_\psi) \approx \int_0^1 dz d\hat{\sigma}_{A+B \rightarrow g+X}(\hat{p}/z, \mu_F) D_{g \rightarrow J/\psi}(z, \mu_F), \quad (14)$$

where  $d\hat{\sigma}_{A+B \rightarrow g+X}$  is the partonic production cross section for hadrons  $A$  and  $B$  to produce parton  $g$ ,  $p_\psi$  is the momentum of  $J/\psi$ ,  $\hat{p}^\mu = (p_\psi^+, 0, 0_\perp)$ ,  $z$  is the  $J/\psi$  momentum fraction. In NRQCD, the fragmentation function  $D$  can be further factorized as

$$D_{g \rightarrow J/\psi}(z, \mu_F) = \sum_n d_{g \rightarrow c\bar{c}[n]}(z, \mu_F) \langle \mathcal{O}^{J/\psi}(n) \rangle, \quad (15)$$

where  $d_{g \rightarrow c\bar{c}[n]}$  can be calculated perturbatively. The dominant channels are  $n = 1S_0^{[8]}$ ,  $3S_1^{[8]}$ ,  $3P_J^{[8]}$ , where the  $n = 1S_0^{[8]}$  and  $3P_J^{[8]}$  contribute leadingly in  $\alpha_s$  to the  $\Sigma_{P.T.}(\cos \chi)$  by emitting one hard gluon, while the soft radiation in the  $3S_1^{[8]}$  channel constitutes the major part of the  $\Sigma_{N.P.}(\cos \chi)$ .

At LO in  $\alpha_s$ , one hard gluon is emitted in  $1S_0^{[8]}$  and  $3P_J^{[8]}$  channels and we have

$$d_{g \rightarrow c\bar{c}[n]}^{\text{LO}}(z, \mu_F) = \int ds \hat{d}_{g \rightarrow c\bar{c}[n]}(z, s, \mu_F). \quad (16)$$

Where  $s = (p_\psi + k)^2$  and  $k$  denotes the momentum of the hard gluon. Then the  $J/\psi$  energy correlator due to the hard gluon reads

$$\begin{aligned} \Sigma_{P.T.}(\cos \chi) &= \frac{1}{M} \sum_n \int_0^1 dz d\hat{\sigma}_{A+B \rightarrow g+X}(\hat{p}/z, \mu_F) \int ds \frac{k \cdot p_\psi}{2m_c} \\ &\times \hat{d}_{g \rightarrow c\bar{c}[n]}(z, s, \mu_F) \delta\left(\cos \chi - \frac{2\sqrt{2}m_c k^+}{k \cdot p_\psi} + 1\right) \langle \mathcal{O}^{J/\psi}(n) \rangle. \end{aligned} \quad (17)$$

Here we focus on the region in which  $\cos \chi > 0$  and therefore we ignore the contribution from a parton in  $\hat{\sigma}_{A+B \rightarrow g+X}$  to hit the detector. A complete calculation will be presented in a future work. Now, using  $s = (p_\psi + k)^2$  and  $k^+ = p_\psi^+(1-z)/z$ , we can rewrite  $\Sigma_{P.T.}(\cos \chi)$  as

$$\Sigma_{P.T.}(\cos \chi) = \sum_n \int_0^1 dz d\hat{\sigma}_{A+B \rightarrow g+X}(\hat{p}/z, \mu_F) \hat{D}_{g \rightarrow c\bar{c}[n]}(z, \cos \chi, \mu_F) \langle \mathcal{O}^{J/\psi}(n) \rangle, \quad (18)$$

with

$$\hat{D}_{g \rightarrow c\bar{c}[n]}(z, \cos \chi, \mu_F) = \frac{2}{M} \int d(k \cdot p_\psi) \left( \frac{k \cdot p_\psi}{2m_c} \right)^3 \frac{z}{1-z} \hat{d}_{g \rightarrow c\bar{c}[n]}(z, k \cdot p_\psi, \mu_F) \delta\left(k \cdot p_\psi - \frac{4m_c^2}{1 + \cos \chi} \frac{1-z}{z}\right). \quad (19)$$

For  $n = 1S_0^{[8]}$  and  $3P_J^{[8]}$ , we find

$$\begin{aligned} \hat{D}_{g \rightarrow c\bar{c}[1S_0^{[8]}]}(z, y, \mu_F) &= \frac{5\alpha_s^2}{16} \frac{1}{6m_c^3} \frac{1}{(y+1)((y-1)z+2)^2} \times \left( (y-1)^2 z^2 + 2(y-1)z + 2 \right), \\ \hat{D}_{g \rightarrow c\bar{c}[3P_J^{[8]}]}(z, y, \mu_F) &= \frac{5\alpha_s^2}{16} \frac{1}{6m_c^5} \frac{1}{(y+1)((y-1)z+2)^2} \times \left( -2(y^3 - 10y + 9)z^3 + (3y^2 - 14y + 25)z^2 \right) \end{aligned} \quad (20)$$

$$+ (y-1)^2(2y+5)z^4 + 2(5y-7)z + 6), \quad (21)$$

with  $y = \cos \chi$ . Inserting the above results into Eq. (18), we obtain the  $\Sigma_{P.T.}$ .

For  ${}^3S_1^{[8]}$ , we write

$$\Sigma_{N.P.}(\cos \chi) = \int_0^1 dz d\hat{\sigma}_{A+B \rightarrow g+X}(\hat{p}/z, \mu_F) \hat{D}_{g \rightarrow c\bar{c}[{}^3S_1^{[8]}]}(z, \cos \chi, \mu_F) \langle \mathcal{O}^{J/\psi}({}^3S_1^{[8]}) \rangle, \quad (22)$$

where

$$\hat{D}_{g \rightarrow c\bar{c}[{}^3S_1^{[8]}]}(z, \cos \chi, \mu_F) = \int d\Phi_{gg} \frac{2k_1^0}{M} \delta(\cos \chi - \cos \theta) \sum_{\lambda} d_{g \rightarrow c\bar{c}[{}^3S_{1,\lambda}^{[8]}]}^{\text{LO}}(z, \mu_F) \frac{A_{\lambda}^{3S_1^{[8]}}(\theta, \phi)}{\langle \mathcal{O}^{J/\psi}({}^3S_1^{[8]}) \rangle}, \quad (23)$$

here  $d\Phi_{gg}$  is the phase space for two gluons emitted,  $A_{\lambda}^{3S_1^{[8]}}$  denote the transition amplitude for  $c\bar{c}[{}^3S_{1,\lambda}^{[8]}] \rightarrow J/\psi + gg$ , and  $\theta$  and  $\phi$  are the polar and azimuthal angles of one of the emitted soft gluons in the helicity frame of  $J/\psi$ .  $k_i$  ( $i = 1, 2$ ) represent the momentum of emitted gluons.

At the leading order of  $v$ , the  $c\bar{c}[{}^3S_{1,\lambda}^{[8]}]$  pair will be transmitted into  $J/\psi$  via two  $E_1$  gluon emissions. Using the heavy quark spin symmetry, we find  $A_{\lambda}^{3S_1^{[8]}}(\theta, \phi)$  is also independent of  $\theta$  and  $\phi$ . Therefore, we have

$$A_{\lambda}^{3S_1^{[8]}}(\theta, \phi) = \frac{1}{4\pi} \frac{1}{3} G_2, \quad (24)$$

where  $G_2$  is a solid angle independent function and satisfies  $\frac{1}{4\pi} \int d\Phi_{gg} G_2 \sim \mathcal{O}(\langle \mathcal{O}^{J/\psi}({}^3S_1^{[8]}) \rangle)$ . Inserting Eq. (24) into Eq. (23), we derive

$$\begin{aligned} \hat{D}_{g \rightarrow c\bar{c}[{}^3S_1^{[8]}]}(z, \cos \chi, \mu_F) &= \int d\Phi_{gg} \frac{G_2}{4\pi} \frac{2k_1^0}{M} \delta(\cos \chi - \cos \theta) d_{g \rightarrow c\bar{c}[{}^3S_1^{[8]}]}^{\text{LO}}(z, \mu_F) \frac{1}{\langle \mathcal{O}^{J/\psi}({}^3S_1^{[8]}) \rangle} \\ &\equiv \bar{v}_2 \times \frac{1}{2} d_{g \rightarrow c\bar{c}[{}^3S_1^{[8]}]}^{\text{LO}}(z, \mu_F), \end{aligned} \quad (25)$$

here  $m_c \bar{v}_2$  is the average energy of one of the emitted soft gluons. And

$$d_{g \rightarrow c\bar{c}[{}^3S_1^{[8]}]}^{\text{LO}}(z, \mu_F) = \frac{\pi \alpha_s}{24 m_c^3} \delta(1-z). \quad (26)$$

Using Eqs. (22) and (25), we can find the  $\Sigma_{N.P.}$ .